Pt/Co(0001) superstructures in the submonolayer range: A tight-binding quenched-molecular-dynamics study

C. Goyhenex, H. Bulou, and J.-P. Deville
Institut de Physique et Chimie des Matériaux de Strasbourg, UMR 7504, 23 rue du Loess, F-67037 Strasbourg Cedex, France

G. Tréglia
CRMC2-CNRS, Campus de Luminy, Case 913, F-13288 Marseille Cedex 09, France
(Received 6 October 1998; revised manuscript received 1 April 1999)

We determine here the most stable structures of a Pt deposit onto a Co(0001) substrate, in the submonolayer range, by means of tight-binding quenched-molecular-dynamics simulations. Our essential result is that Pt/Co growth is essentially governed by the strain imposed by the substrate and by the tendency of the adatoms to avoid *on-top* positions. More precisely, whereas in the first stages of Pt deposition the strong adsorbate-substrate interaction leads to the formation of a high density of strained islands, these islands are able to relax before completion of the first monolayer (0.8 ML), thanks to the incorporation of Co atoms removed from the substrate. This phenomenon can be viewed as a first step towards the formation of a *size-mismatch-induced surface alloy*, in full agreement with photoemission spectroscopy experiments. [S0163-1829(99)07527-X]

I. INTRODUCTION

The properties of heteroepitaxial systems, among which is magnetism, are strongly dependent on the structural and the chemical nature of the interface. In most cases, this interface is far from being a perfectly flat and abrupt one, even in the absence of interdiffusion and especially when the two elements (deposit, substrate) present a strong size mismatch. Generally, simple wetting arguments, based on the difference in surface energies between both elements and on their mixing ability that drives the interfacial energy, are not sufficient to predict the growth modes in the submonolayer range. It is then essential to understand and possibly to model how the system releases the strain induced by the size mismatch, through atomic relaxation and reconstruction of the interface as a function of coverage. This is only possible by performing systematic studies for well-defined systems, on both experimental and theoretical sides. Pt/Co is a good candidate for such studies since the two elements present a large size mismatch (11%), almost the same surface energy ($\Delta\gamma = 1.8\%$), and a tendency to chemical order as evidenced by the corresponding bulk phase diagram. From an applied point of view, this system has been widely studied for its magnetic properties.

Platinum on Co(0001) shows a three-dimensional (3D) growth mode as evidenced by means of synchrotron-induced core-level photoemission spectroscopy and Monte Carlo simulations.[1] Strained epitaxial layers in a twinned-fcc structure have been observed by means of grazing incidence x-ray scattering.[2] From the theoretical point of view, developing a microscopic model, which should be able at the same time to account for strain release, via atomic relaxations and reconstructions, and for possible chemical rearrangements, is necessary.

Our purpose is to model the first stages of Pt deposition in the simplest way, i.e., by determining the most stable equilibrium positions of these atoms as a function of the coverage, at 0 K. One needs to relax individually both adatoms and substrate atoms that occupy inequivalent positions. This can be done in the framework of a quenched-molecular-dynamics simulation, provided one uses many-body potentials sufficiently realistic to account for surface relaxations. The present work is devoted to the equilibrium structure of a Pt deposit on Co(0001). The principles of the numerical simulations and the derivation of the tight-binding potentials are described in Sec. II. The superstructures of Pt deposits on Co(0001) are presented as a function of coverage in Sec. III. They are followed by a discussion and a comparison with experiments (Sec. III D).

II. THEORETICAL MODEL

A. Quenched-molecular-dynamics (QMD) method

QMD is a relaxation procedure that allows one to determine the equilibrium structure of a system, at $T=0$ K, by integrating the equation of motion,[3]

$$F_i = m_i \frac{dv_i}{dt}, \tag{1}$$

where $v_i(t)$ is the velocity at time t of an atom at site i with mass m_i, and $F_i(t)$ is the force acting on this atom.[4] A quenching procedure which consists of canceling v_i when the product $F_i(t)v_i(t)$ becomes negative has been applied. The force on the atom at site i is obtained from

$$F_i = -\frac{dE_{tot}}{dr_i}, \tag{2}$$

with

$$E_{tot} = \sum_i E_i, \tag{3}$$

where E_i is the energy of this atom. Calculating this energy then requires the knowledge of Pt-Pt, Co-Co, and Pt-Co interactions.

B. Derivation of the interatomic potentials for the Pt-Co system

In the tight-binding formalism,[5] the energy of an atom at site i is written as the sum of two terms, an attractive band energy and a repulsive pair interaction:

$$E_i = E_i^b + E_i^r . \tag{4}$$

The band term is obtained by integrating the local density of states up to the Fermi level,[5] which gives rise to the many-body character of the potentials necessary to account for surface relaxations and reconstructions.[6] When replacing the realistic density of states by a schematic rectangular one having the same second moment, i.e., the same full width at half maximum (*second-moment approximation*[7]), one obtains

$$E_i^b = -\left\{ \sum_{j, r_{ij} < r_c} \xi_{IJ}^2 \exp\left[-2q_{IJ}\left(\frac{r_{ij}}{r_0^{IJ}} - 1 \right) \right] \right\}^{1/2} . \tag{5}$$

The exponent q_{IJ} characterizes the distance dependence of the hopping integral between atoms at sites i and j. ξ_{IJ} is an effective hopping integral. I and J indicate the chemical species: $\{I,J\} = \{\text{Co or Pt}\}$, r_0^{II} is the first-neighbor distance in the metal I and $r_0^{IJ} = (r_0^{II} + r_0^{JJ})+/+2$. The interaction is canceled beyond a cutoff radius r_c.

The repulsive term E_i^r is described by a sum of Born-Mayer ion-ion repulsions:[8]

$$E_i^r = \sum_{j, r_{ij} < r_c} A_{IJ} \exp\left[-p_{IJ}\left(\frac{r_{ij}}{r_0^{IJ}} - 1 \right) \right], \tag{6}$$

where p_{IJ} is related to the bulk modulus of the metal.

For each pure metal species (Pt, Co), the parameters (ξ, A, p, q) are determined by fitting the potential to the universal equation of state driving the variation of the potential with distance.[9,10] This procedure implies that the experimental values of the cohesive energy, lattice parameter, and bulk modulus are known. This is the case for Pt and Co.[11] To use the same cutoff radius for both metals, r_c has been fixed at the second-neighbor distance for the largest atom, i.e., Pt. From r_c up to the (Co-Co) third-neighbor distance, the potential is linked up to zero with a fifth-order polynomial to avoid discontinuities both in the energies and in the forces. The cutoff was not extended to the fifth neighbors as done in Ref. 12 within the same formalism since the computational time due to this long-range interaction is too important with regard to the small improvement that this could bring. Fitting the universal equation leads to the following values of the parameters: $p = 11.14$, $q = 3.68$, $A = 0.242$ eV, $\xi = 2.506$ eV for Pt and $p = 8.80$, $q = 2.96$, $A = 0.189$ eV, $\xi = 1.907$ eV for Co.

A well-known problem of this fitting procedure is that it leads to underestimated surface energies, as it can be seen from their comparison with the experimental ones:[13]

$$\gamma_{\text{Pt}}^{cal} = 0.46 \text{ eV/atom}, \quad \gamma_{\text{Co}}^{cal} = 0.35 \text{ eV/atom},$$

$$\gamma_{\text{Pt}}^{expt} = 1.03 \text{ eV/atom}, \quad \gamma_{\text{Co}}^{expt} = 0.87 \text{ eV/atom}.$$

This drawback is not too serious since it has been shown that when interested in bimetallic surface problems (segregation, deposition) the quantity that has to be preserved is not the surface energy of each element, but the difference between them.[14] Here this difference is well reproduced:

$$\Delta\gamma^{cal} = 0.11 \text{ eV/atom}, \quad \Delta\gamma^{expt} = 0.15 \text{ eV/atom}.$$

The main requirement for the cross-interaction parameters is to properly account for the tendency to bulk ordering, i.e., favoring heteroatomic pairs. This is achieved by fitting the experimental heats of dissolution of one impurity of Pt in Co (respectively, Co in Pt). This can be obtained from the slopes of the mixing energies[15] in the dilute limits, with $E_{sol} = -0.47$ eV/atom for Pt (Co) and $E_{sol} = -0.65$ eV/atom for Co (Pt).

It is worth noticing that, due to the large size mismatch between Co and Pt, the whole system (matrix+impurity) has to be relaxed during the fitting procedure. Having only two equations for four parameters, only two of them (A and ξ) are left free while p and q are taken as the arithmetic average between the pure metal values. Doing this, one finds $p = 9.97$, $q = 3.32$, $A = 0.245$ eV, $\xi = 2.386$ eV for Pt-Co interactions.

The use of such semiempirical potentials is indeed approximate but gives a reasonable description of the transition close-packed metals and particularly allows simulations with thousands of atoms. A realistic *ab initio* calculation in the same conditions is out of range of possibilities.

C. Relative stabilities of the obtained structures

In order to compare the relative stabilities of the different structures an energy criterion is necessary to ascribe the most stable structure to the lowest energy. To this aim, when one deposits n_s Pt atoms onto a Co substrate with N_s atoms per plane, corresponding to a coverage $\theta = n_s/N_s$ ML, one defines the adsorption energy per Pt atom as follows:[16]

$$E_{ads}(\theta) = \frac{E_{tot}(A/B) - E_{tot}(B) - n_s\mu(A)}{n_s}, \tag{7}$$

where $E_{tot}(A/B)$ is the total energy (Co substrate and n_s adsorbed Pt atoms), and $E_{tot}(B)$ is the energy of the bare substrate, which writes for a slab of k layers

$$E_{tot}(B) = kN_sE_{coh}(B) + N_sE_{surf}(B). \tag{8}$$

$\mu(A)$ is the chemical potential of the Pt vapor phase taken as the origin of energies.

III. STRUCTURE OF A Pt DEPOSIT ON A Co(0001) SUBSTRATE

The quenching procedure allows one to reach any local energetic minimum, but does not guarantee that it is the lowest one. However, it allows one to determine a full energetic map through the identification of these local minima, which can exchange their respective stabilities upon external pa-

rameters (temperature, coverage). Therefore, to avoid being blocked in one minimum of secondary importance, and to reveal the most significant ones, one has either to perform simulated annealings or to start from a sufficiently large set of initial configurations to explore the whole configuration space. The second solution was chosen, and the tight-binding QMD (TBQMD) simulations were performed starting with three different realistic configurations.

(i) A Pt island in registry with the Co substrate, the n_s Pt atoms being separated by a Co-Co distance (contraction).

(ii) A Pt island in which the n_s Pt atoms keep their bulk Pt-Pt separation.

(iii) $n \times n$ pseudoepitaxial superstructure ($n = \sqrt{n_s}$), where the n_s Pt atoms are homogeneously distributed upon the surface of the Co substrate. In the submonolayer range, configurations (i) and (ii) allow one to describe isolated islands and configuration (iii) corresponds only to a continuous superstructure. The misfit between Co and Pt being $\Delta r/r = 0.1$, configurations (ii) and (iii) are equivalent for $\theta = (9 \times 9)/(10 \times 10) = 0.81$ ML, which corresponds to a pure Pt(111) plane onto a Co(0001) plane, both layers keeping, respectively, their bulk distances. To stabilize such a superstructure in a simulation, one has to impose a lateral size which is a multiple of 10 since, due to the finite size of the simulation boxes, this superstructure is repeated laterally according periodic conditions. Perpendicularly to the surface, no periodic conditions are applied so that one deals with a slab thick enough (typically 10 atomic layers) to recover the bulk properties in the midlayer.[17] To accommodate the size mismatch, one has to use boxes containing N Co atoms and $n = N + \Delta n$ Pt atoms along the dense $\langle 110 \rangle$ rows with

$$N = \frac{\Delta n}{r^* - 1}, \tag{9}$$

where the ratio of Co to Pt atomic radii $r^* = 0.902$. The first two solutions, corresponding, respectively, to $\Delta n = -1$ (one row removed) and $\Delta n = -2$ (two rows removed), lead to values of N either between 10 and 11, or between 20 and 21. Changing the coverage and/or the compactness of the Pt deposit corresponds to a variation of Δn. Figure 1 shows an overview of the variation of the adsorption energy per Pt atom obtained as a function of the coverage in the range 0.0–1.0 ML for a simulation cell containing 20 Co atoms along $\langle 110 \rangle$. We had to change the size cell only in the case of configuration (iii) in order to vary more finely the compactness of the Pt layer for coverages around 0.81 ML.

For each point of these curves, it has been possible to derive the function that gives the distribution of distances around one atom after relaxation of the structures, and then by averaging on all sites to derive the *mean shortest* distance between the Pt atoms. The variation of this Pt-Pt shortest distance with coverage is plotted in Fig. 2. Note that one has also access to the Co-Pt shortest distance at the interface, but it does not vary in a noticeable way around 2.59 Å for all the investigated structures and coverages. This indicates a vertical inwards relaxation of about 2% with respect to a hard-sphere stacking using the bulk neighbor distances.

The minimal energy $E_{ads} = -5.94$ eV/atom is obtained for a pseudoepitaxial layer with a (12×12) periodicity at $\theta = 0.84$ ML. With an average lateral contraction of 1.5%, this

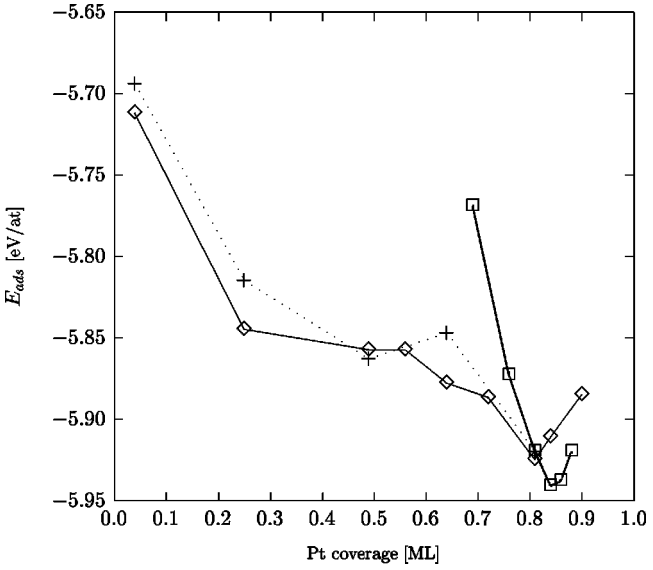

FIG. 1. Variation of the adsorption energy with Pt coverage. ◇, result of the relaxation of configuration (i), i.e., island with an initial interatomic shortest distance $R_{\mathrm{Pt}}^{init} = 2.50$ Å. +, result of the relaxation of configuration (ii), i.e., island with $R_{\mathrm{Pt}}^{init} = 2.77$ Å. □, result of the relaxation of pseudoepitaxial layers [initial configuration (iii)].

superstructure is found slightly more close packed than a Pt bulk (111) plane. This means that the completion of the first monolayer as defined earlier, which would correspond to the first break point in the Auger spectrum, is achieved for $\theta = 0.84$ ML. Then, by continuing to add atoms in the first layer beyond 0.84 ML, the structure becomes more and more compressed and the corresponding adsorption energy increases rapidly, up to a dramatically high energy for $\theta = 1.0$ ML: $E_{ads}(1.0\ \mathrm{ML}) = -5.37$ eV/atom (out of the figure scale). A coherent epitaxy is highly unfavorable and the second layer should start growing beyond 0.84 ML. When going to lower coverages, both initial configurations (i) and (ii)

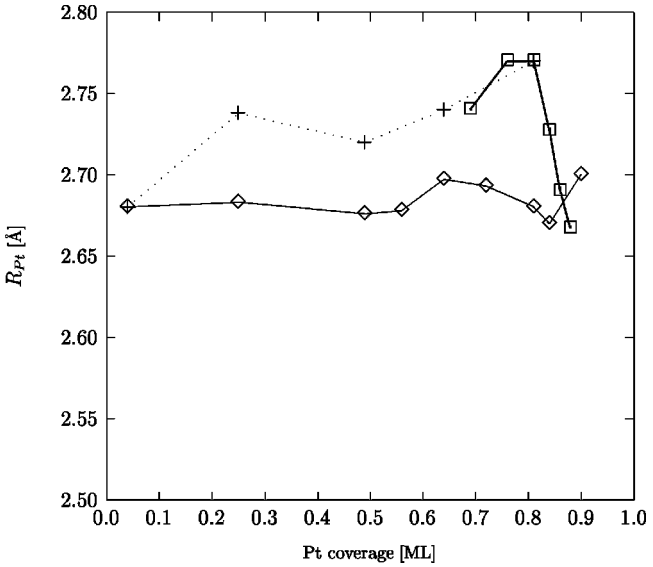

FIG. 2. Pt-Pt mean shortest distances. ◇, initial configuration (i) ($R_{\mathrm{Pt}}^{init} = 2.50$ Å). +, initial configuration (ii) ($R_{\mathrm{Pt}}^{init} = 2.77$ Å). □, initial configuration (iii) (pseudoepitaxial layers).

lead to higher energies. Even though the energy curves obtained in both cases present a similar behavior and are close together, the corresponding distances appear as rather different, depending on the initial configuration. More precisely, the average shortest distance remains smaller when starting from the Co-Co bulk configuration [configuration (i)] than from the Pt-Pt one [configurations (ii) and (iii) around 0.8 ML]. In fact, it seems that the two initial structures tend to relax towards a unique stable structure, but are ''blocked'' in some intermediate local minimum, very close to the lowest one. Anyway, this average relaxed distance is always around 2.7 Å, i.e., significantly larger than the Co-Co distance (2.5 Å) and close to the Pt-Pt one (2.77 Å). Below 0.84 ML, the deposit should be constituted of islands reconstructed according to the (12×12) optimal superstructure, which should then appear well below the critical coverage of 0.84 ML. Therefore, the increase of the energy when θ decreases is probably due to an edge effect related to the increasing proportion of edge atoms when the coverage decreases. Due to the finite size of the simulation cells, decreasing the coverage corresponds to the simulation of a smaller and smaller two-dimensional (2D) island with, therefore, a higher and higher proportion of edge atoms. As a given coverage can be either realized by a few large islands or many small ones, a systematic study separating the variation of cluster size and cluster density is hardly feasible with the QMD method and is not presented in this work. It should be done together with simulations of the growth kinetics, e.g., using the kinetic Monte Carlo method.

After this first rough analysis, the only way to go further in the description of the relaxed structures and to precisely give the distance distribution corresponding to the stablest structure one must detail the corresponding atomic positions of the Pt atoms with respect to the underlying Co atoms, in the three coverage regions described above: before, at, and after completion of the first monolayer (i.e., on both sides of $\theta=0.84$ ML).

A. Submonolayer range: $\theta<0.75$ ML

When submitted to the relaxation process, the Pt adatoms move individually in order to satisfy contradictory criteria. Unfavorable positions such as a Pt atom on top of a Co atom should be avoided. The Pt atoms want to keep in registry with the substrate to optimize the Co-Pt interaction, but at the risk of a strong compressive stress in the Pt overlayer. On the other hand, the same Pt lattice should try to recover the bulk interatomic distances to release this compression. The relaxed structures can be viewed as the best way to accommodate these competing requirements. This is illustrated here in the particular case of $\theta=0.64$ ML, in Fig. 3.

When starting with an island in coherent epitaxy [configuration (i): upper panel], all the Pt adatoms occupy equivalent hcp ternary sites with respect to the substrate. Owing to the space left free around the island, the Pt lattice is able to expand under relaxation in order to release the strain induced by this highly symmetrical but very compressed initial configuration. However, as previously mentioned (see Fig. 2), the Pt atoms never recover their bulk interatomic distance but keep an average in-plane relaxation of -2.8%, which can be explained as follows. Trying to recover exactly the bulk separation would lead the Pt adatoms to occupy all the possible inequivalent positions with respect to the Co atoms, including the most unfavorable on-top ones. Stopping the expansion before reaching this state can then be viewed as a possible way to avoid these latter sites. The corresponding adsorption energy is $E_{ads}=-5.878$ eV/atom. On the contrary, when starting from an unstrained island (Fig. 3, lower panel) already presenting the bulk Pt lattice parameter, the situation is somewhat different since some Pt adatoms initially occupy such on-top sites. Therefore, under relaxation, these Pt atoms try to move away from these unfavorable sites, leading to an average in-plane relaxation of -1.5%, but remain trapped close to them, due to the difficulty to perform some more collective displacements. As a consequence, the corresponding adsorption energy is found somewhat higher ($E_{ads}=-5.847$ eV/atom) than in the case of initially more close-packed islands. Anyway, both structures are very similar and can be viewed as slightly contracted (between 1.5% and 2.8%) two-dimensional Pt islands. This analysis still holds in the whole coverage region investigated (from 0.0 to 0.75 ML), for which the deposit should then be constituted of slightly constrained Pt islands, resulting from the strong deposit-substrate interaction which allows, at least in the first stages of the growth, to avoid on-top positions. In fact, as can be guessed from Fig. 3, the distribution of the interatomic distances is not homogeneous. The islands obtained from the configurations (i) have the distribution shown on Fig. 4. It is centered around the mean value of 2.697 Å. The peak at 2.61 Å [also observed for the islands from configurations (ii)] is due to a more pronounced contraction at the islands edges. Such an edge relaxation,

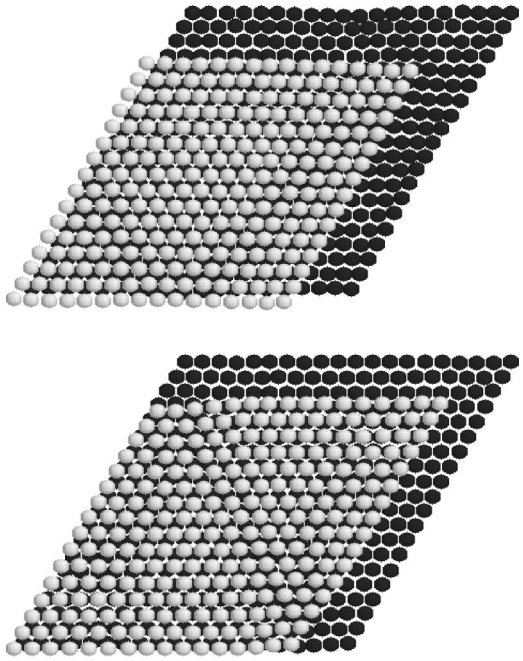

FIG. 3. $\theta=0.64$ ML: top view of the relaxed island structure starting from either configuration (i) (upper panel: $E_{ads}bf=-5.878$ eV/atom; $R^0_{\mathrm{Pt}}=2.697$ Å) or configuration (ii) (lower panel: $E_{ads}=-5.847$ eV/atom; $R^0_{\mathrm{Pt}}=2.74$ Å) initial configuration. The light gray balls represent the Pt adatoms and the dark ones the Co atoms of the first layer of the substrate. They are represented with the same size for the sake of clarity of the atomic positions.

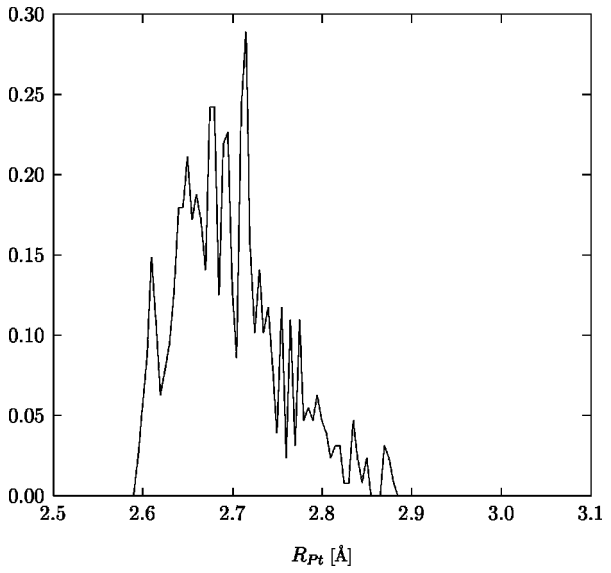

FIG. 4. $\theta = 0.64$ ML: distribution of the lateral distances around Pt atoms in the island obtained from initial configuration (ii).

usually observed in small metal clusters, originates from an inwards relaxation occuring at the surface of these clusters similar to the known relaxation of the extended metallic surfaces.[18] This effect adds to the previous arguments in favor of the formation of slightly contracted Pt islands in the first stages of the growth.

B. Completion of the first monolayer: $0.75 < \theta < 0.85$ ML

When approaching the completion of the first layer the situation becomes more intricate since the on-top positions can no longer be avoided just by reducing the mean interatomic distance. The curves for configurations (ii) have to be terminated at the limit coverage of 0.81 ML since it is not possible to build bulklike Pt islands beyond. Up to this limit, the energy decreases monotonically with increasing coverage to reach its minimum value, $E_{ads} = -5.92$ eV/atom at 0.81 ML. The curves for configurations (i) and (iii) do not present such a limitation so that they can be drawn in the whole coverage range under analysis. Both present a pronounced minimum around 0.81 ML. For configurations (iii), the initial pseudoepitaxial Pt layer is significantly expanded with regard to bulk Pt below 0.81 ML. In that case, the main effect of relaxation is to introduce discontinuities in this layer, leading to the formation of a network of identical islands due to the lateral Pt-Pt interactions which force the adatoms to come closer one with the other. The appearance of several islands per simulation cell strongly increases the proportion of edge atoms, leading to a very high adsorption energy which makes the corresponding structures highly unstable. Therefore, as can be seen on the curve of Fig. 1, relaxed structures derived from (iii) initial configurations are only competing with the others close to the 0.81 ML coverage, for which they optimize the adsorption energy (as soon as the edge effect disappears). The corresponding superstructure is illustrated in Fig. 5. At 0.81 ML, the relaxation does not lead anymore to the formation of islands and the Pt initial lattice is in the main conserved. As for the (ii) case (which is completely equivalent at this coverage) no contraction at all is

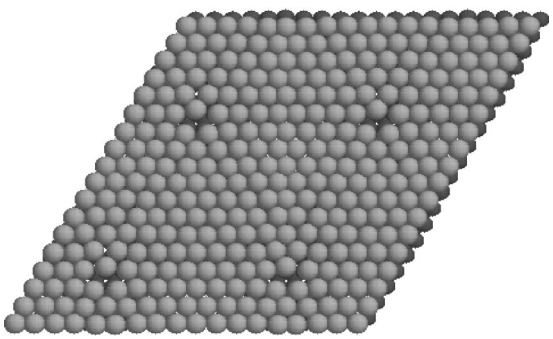

FIG. 5. $\theta = 0.81$ ML: the initial configuration is a pseudoepitaxial layer. $E_{ads} = -5.92$ eV/atom and $R^0_{\mathrm{Pt}} = 2.77$ Å.

observed, contrary to what occurs starting with configuration (i), due once again to the difference between a continuous layer and an islandlike deposit structure. In fact, as can be seen from the quasiholes surrounding the Pt on-top positions, it seems that the Pt layer is still not close packed enough. By increasing the coverage a little bit more, one finds that the minimum adsorption energy is reached for $\theta = 0.84$ ML, corresponding to a (12×12) superstructure which presents an in-plane contraction of 1.5% with respect to bulk Pt. Then beyond 0.84 ML the too strong compression leads to higher adsorption energies, in both the (i) and (iii) cases, even though the latter curve remains slightly lower than the former, probably due to the absence of the edge effect. However, at 0.84 ML, no significant change can be viewed in the structure of the relaxed overlayer compared to that obtained at 0.81 ML and presented in Fig. 5. Indeed, one still observes a local motion of the Pt atoms trying to move away from on-top positions. This feature seems to indicate that even though the energy curve shows a minimum at $\theta = 0.84$ ML, it is perhaps possible to get a better structure by finding some way to allow Pt adatoms to avoid this unfavorable site, other than by keeping the highly unstable positions in registry with the Co lattice. Actually, a close inspection of the profile view of a relaxed Pt islandlike deposit initially in registry with Co will give some indication of a possible way to reach this goal. This view is represented in Fig. 6 for $\theta = 0.81$ ML. The Pt adlayer is rather compressed, since the shortest lateral distance is $R^0_{\mathrm{Pt}} = 2.67$ Å. It induces a strong corrugation that the system tries to release by removing a few Co atoms (about 5%) from the first substrate underlayer up to the edge of the strained Pt islandlike deposit. A detailed analysis of the results shows that such a Co-Pt mixing occurs in the simulations as soon as the critical coverage of $\theta^* = 0.76$ ML is reached. However, this effect only appears when there is enough space around the simulated islandlike deposit, which requires sufficiently large simulation cells to allow large enough absolute value of Δn. So, for the cells with 10 Co atoms along $\langle 110 \rangle$ this phenomenon never appeared. The creation of Co vacancies in the first underlayer can be related to STM observations made on two other systems presenting a similar size mismatch between deposited and substrate atoms, namely, Au/Ni(111) (Ref. 19) and Ag/Cu(111).[20] In both cases, a triangular-shaped periodic corrugation of the adlayer was attributed to the existence of an ordered array of dislocation loops in the substrate, corresponding to local fcc/hcp stacking faults that allow one to avoid the on-top positions. These conclusions were supported by atomistic simu-

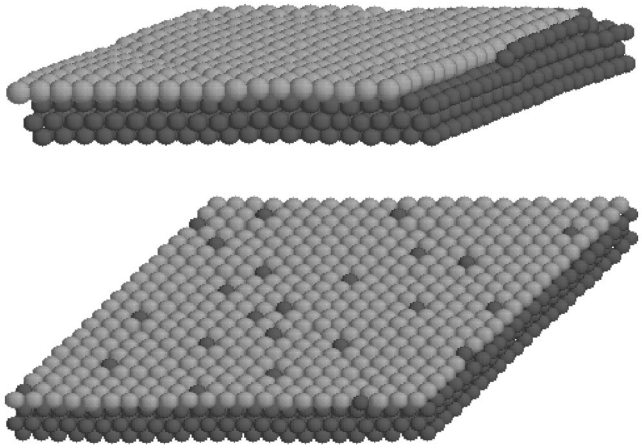

FIG. 6. Profile view of the relaxed structure obtained from configurations (i) (islandlike structure) and (iii) (continuous layer with incorporation of Co atoms from the substrate in the Pt overlayer). Upper part: $\theta=0.81$ ML, $E_{ads}=-5.925$ eV/atom and $R^0_{\mathrm{Pt}}=2.67$ Å; lower part: $\theta=0.80$ ML, $E_{ads}=-5.990$ eV/atom and $R^0_{\mathrm{Pt}}=2.73$ Å.

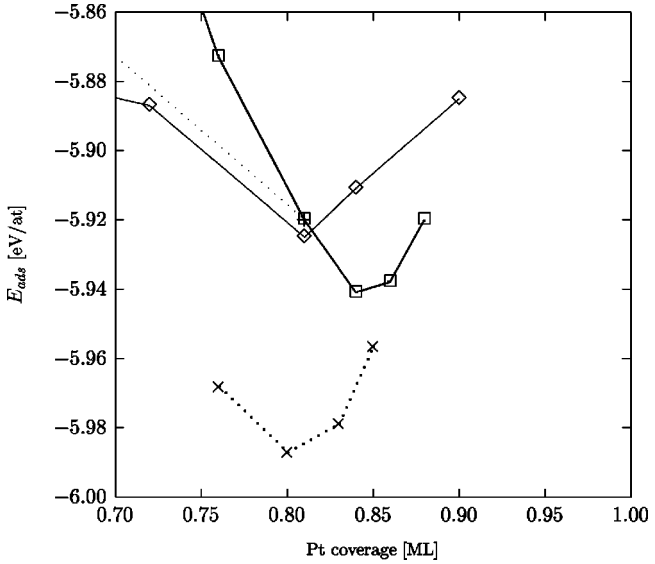

FIG. 7. Variation of the adsorption energy with Pt coverage. ◇, $R^{init}_{\mathrm{Pt}}=2.50$ Å. +, $R^{init}_{\mathrm{Pt}}=2.77$ Å. □, continuous pseudoepitaxial layer. ×, continuous pseudoepitaxial layer with incorporation of Co atoms from the substrate.

lations performed, respectively, within the effective-medium theory for Au/Ni(111) (Ref. 19) and the tight-binding formalism for Ag/Cu(111).[20] A main difference between both systems was that the removed Ni atoms were incorporated in the Au adlayer but not the Cu atoms in the Ag one. The simulations suggest that our case is more similar to the Au/Ni one, with the additional information that this mixing should occur preferentially at the edges of Pt islands. This enhanced surface mixing can be understood as resulting from the tendency to favor heteroatomic pairs instead of homoatomic ones in the bulk Pt-Co system and the possibility to release the strain energy associated to the existence of on-top sites by the creation of a hcp/fcc stacking fault in the first substrate layer. In order to *help* the relaxation process to better optimize the Co atom removal, a series of simulations has been performed in which we started from the continuous superstructures (iii), in which we have incorporated a variable number of Co atoms removed from the substrate first layer. The choice of the Co atoms to be removed was made in order to allow the Pt atoms initially located in on-top positions to relax more easily towards *ternary* ones. The number of Pt atoms in the layer (i.e., the coverage) was varied by using unit cells of Co such as $20\leqslant N\leqslant 30$ and $\Delta n=-2$. When starting with the (12×12) superstructure, four rows of six Co atoms were removed from the substrate, creating 5% vacancies in the underlying Co plane as suggested by the ejections observed during our first simulations (see the upper part of Fig. 6). These vacancy rows allowed one to shift four triangles of 15 Co atoms from a hcp toward a fcc stacking, forming a substrate partial dislocation loop. In order to create this hcp/fcc stacking fault in the first layer of the initially hcp Co crystal the orientation of the loops has to be up. On the contrary, in the cases of Ni and Cu fcc substrates the orientation of the observed loops was down since the stacking fault has occurred in the direction fcc towards hcp.

The removed Co atoms were then incorporated in the Pt overlayer. Under relaxation the interface rearranged itself in order to give the relaxed structure shown in the lower part of Fig. 6 and which can be viewed as a first step towards a *surface alloy* formation. Note that this case corresponds to a slight decrease of the coverage: $\theta=0.80$ ML instead of $\theta=0.81$ ML. The corresponding adsorption energy is then clearly improved. In Fig. 6 Co atoms are alloyed in the Pt overlayer with a maximum of heteroatomic bonds (a Co atom being surrounded by six Pt atoms in the plane) which corresponds to the lowest energy cost to incorporate the Co atoms into the Pt deposit. In Fig. 7 are reported the adsorption energy values obtained in the coverage range 0.76–0.85 ML. The minimal energy $E_{ads}=-5.990$ eV/atom, found for the optimal coverage of 0.80 ML, corresponds to an optimal proportion of 5% alloyed Co atoms. The mean lateral lattice parameter is then $R^0_{\mathrm{Pt}}=2.73$ Å.

C. Beyond the completion: $0.85<\theta\leqslant 1.00$ ML

Starting from an initial coherent epitaxy at $\theta=1.00$ ML, the TBQMD relaxation does not allow the system to leave this highly symmetrical configuration. The associated adsorption energy is therefore very high: $E_{ads}(1.00\ \mathrm{ML})=-5.37$ eV/atom. In order to break the symmetry of the coherent epitaxy, a simulated annealing of this configuration was performed. An initial temperature of $T=500$ K is sufficient to eject atoms from the compact Pt layer, allowing the Pt lattice to expand (up to 2.74 Å). This ejection mechanism, known as the size-mismatch-induced limited ejections (SMILE) effect,[21] allows one to strongly lower the final adsorption energy ($E_{ads}=-5.82$ eV/atom), but not sufficiently to reach the minimum region. Already from $\theta=0.90$ ML, some Pt atoms are ejected on top of the first Pt adlayer due to the SMILE effect, which allows to define a limiting value for the lateral contraction supported by the Pt lattice: $R_0^{limit}(\text{Pt-Pt})=2.67$ Å.

D. Discussion and comparison with the experiments

From the experimental point of view, the growth and structure of Pt/Co(0001) at room temperature have been ex-

tensively investigated using a large panel of surface techniques. The crystallographic structure of the Pt layers was resolved by mean of grazing incidence x-ray scattering (GIXS).[2] Actually, the knowledge of the lattice parameter, as well as its evolution versus the coverage, can be viewed as a significant signature of the strain induced by the growth of mismatched films. Experimentally, the Pt films are found in-plane strained up to 2.0 ML, with a constant average lattice parameter of 2.632 ± 0.001 Å reflecting a strong deposit-substrate interaction (above 2.0 ML, the lattice parameter steadily increases up to 2.719 ± 0.001 Å at 10 ML).

These results are consistent with the TBQMD simulations which predict an average lateral lattice parameter of 2.67 Å when 2D islands are simulated in the submonolayer coverage. Note that the experimental and theoretical results could not directly be compared since the experimentally Pt thickness was estimated from the intensity attenuation of the Auger Co *MVV* peak assuming a layer-by-layer growth mode. Because of the 3D growth mode of Pt/Co(0001), the experimental coverage is overestimated with respect to the one used in the simulations. Thus, it is reasonable to think that the completion of the first layer occurs for an experimentally estimated Pt thickness of about 2 ML, consistent with the 3D growth mode of Pt on Co(0001). The slight discrepancy which appears between the theoretical and experimental lattice parameters could be due to several factors. One of the most important is without any doubt the possibility of a nucleation of platinum islands at cobalt edges, a situation not included in the calculations. In this case, an additional strain is imposed to the platinum atoms, which can probably contribute to the decrease of the lattice parameter. Nevertheless, in the light of the simulations, we can say that the formation of a high density of small strained islands, deduced from the experiments, can be viewed as the way with the lowest energy cost to avoid on-top positions.

The chemical structure of the interface was investigated by means of synchrotron-induced core-level photoemission spectroscopy[1] on the Pt $4f_{7/2}$ line. Using Monte Carlo simulations in order to reproduce the experimental intensities of the Pt $4f_{7/2}$ photoemission line versus Pt thickness, evidence was found that small islands yielding a high nucleation density grow on top of the substrate, confirming previous Auger electron spectroscopy (AES) results.[22] In addition, this study highlighted the existence of an elementary photoemission line characteristic of platinum atoms embedded in a cobalt-rich environment. This elementary photoemission line appears for a platinum thickness comprised between 2.0 and 3.0 ML and coexists with the pure platinum elementary photoemission line. Thanks to the TBQMD simulations, we propose elements in favor of an enhanced Pt-Co mixing in the Pt overlayer, which should occur preferentially at the edges of the islands, as shown by the removal of the Co atoms from the substrate towards the deposit evidenced by the molecular-dynamics calculations. When the island size increases, while keeping Pt-Pt interatomic distances significantly larger than the Co-Co ones, the interface energy also strongly increases due to the arrival of some Pt atoms in on-top positions. The easiest way to avoid such unfavorable positions is to remove some Co atoms from the substrate and to incorporate them in the first Pt layer. This effect is increased by the twinned-fcc structure of the Pt film.[2] Indeed not only does this structure allow one to form a natural space between the islands with a different orientation (space which is necessary in order that the effect appears—see Sec. III B) but also it involves an area between islands, very unstable from an energetic point of view because of the structural uncompatibility between the *ABC* and *ACB* stackings. Such a surface enhanced mixing, which is a first step towards the formation of a *surface alloy*, is preferred to a simpler superstructure, due to the tendency of this system to favor the formation of heteroatomic bonds and to the very weak hcp/fcc stacking fault energy in Co.[23]

IV. CONCLUSION

Putting together the simulations and the various experimental results, we can derive the following outline for the first stages of Pt deposition on Co(0001). In the earliest stages of the deposition the strong interaction adsorbate-substrate leads to the formation of strained islands. In that case, the growth of a high density of small contracted islands is probably the best way for the Pt adatoms to avoid on-top positions, while keeping interatomic distances significantly larger than the Co-Co ones. Here, more than the usual wetting criterion generally used to describe the growth modes (which involves differences in surface energies which are almost negligible here), the structural strain imposed by the substrate and the tendency of the adatoms to avoid the most unfavorable positions govern the whole process. Then, when the islands extend themselves, avoiding these positions while keeping *bulklike* Pt-Pt distances becomes only possible by removing Co atoms from the substrate into the Pt adlayer. This can be viewed as a first step towards the formation of a *size-mismatch-induced surface alloy* with a characteristic coverage of $\theta = 0.80$ ML and an optimal concentration of Co atoms in the surface alloy of 5%. In this condition the Pt lattice is able to release more easily, the lateral shortest interatomic distance being $R^0_{\mathrm{Pt}} = 2.73$ Å. It would now be interesting to check experimentally this surface alloy formation by STM as it was done to evidence the correlated dislocation loops in the substrate for Au/Ni and Ag/Cu. At the moment, this is hindered by the difficulty in preparing Co surfaces exhibiting only hcp(0001) domains. However, the recent results obtained by GIXS on Pt/Co(0001) prove the possibility of obtaining high quality Co surfaces and are therefore encouraging further STM studies of heteroepitaxial growth on a Co substrate, as confirmed by a first STM study of the early stages of growth of Cu/Co(0001).[24] On the theoretical side, the next step should now be to increase the thickness of the deposit and to study the reversed case (Co/Pt) in order to better characterize the influence of the size mismatch on the structure of the deposited film. Some work is in progress in these two directions.

[1] H. Bulou, A. Barbier, R. Belkhou, C. Guillot, B. Carriére, and J. P. Deville, Surf. Sci. **352-354**, 828 (1996).
[2] H. Bulou, A. Barbier, G. Renaud, B. Carriére, R. Baudoing-Savois, and J. P. Deville, Surf. Sci. **377-379**, 90 (1997).
[3] C. H. Bennett, in *Diffusion in Solids, Recent Developments*, edited by A. S. Nowick and J. J. Burton (Academic, New York, 1975), p. 73.
[4] L. Verlet, Phys. Rev. **159**, 98 (1967).
[5] J. Friedel, in *The Physics of Metals*, edited by J. M. Ziman (Cambridge University Press, Cambridge, 1969), p. 340.
[6] B. Legrand, M. Guillopé, J. S. Luo, and G. Tréglia, Vacuum **41**, 311 (1990).
[7] V. Rosato, M. Guillopé, and B. Legrand, Philos. Mag. A **59**, 321 (1989).
[8] F. Ducastelle, J. Phys. (Paris) **31**, 1055 (1970).
[9] J. R. Smith, J. Ferrante, and J. H. Rose, Phys. Rev. B **25**, 1419 (1982).
[10] D. Spanjaard and M. C. Desjonquéres, Phys. Rev. B **30**, 4822 (1984).
[11] C. Kittel, *Introduction to Solid State Physics* (Wiley, New York, 1976).
[12] F. Cleri and V. Rosato, Phys. Rev. B **48**, 22 (1993).
[13] F. R. de Boer, R. Boom, W. C. M. Mattens, A. R. Miedema, and A. K. Niessen, *Cohesion in Metals* (North-Holland, Amsterdam, 1988), Vol. 1.
[14] G. Tréglia, B. Legrand, and F. Ducastelle, Europhys. Lett. **7**, 575 (1988).
[15] R. Hultgren, P. D. Desay, D. T. Hawkins, M. Gleiser, K. K. Kelley, and D. D. Wagman, *Selected Values of Thermodynamic Properties of the Elements* (American Society of Metals, Cleveland, 1973).
[16] C. M. Gilmore, J. A. Sprague, J. M. Eridon, and V. Provenzano, Surf. Sci. **218**, 26 (1989).
[17] V. Rosato, G. Ciccoti, and V. Pontikis, Phys. Rev. B **33**, 1860 (1986).
[18] R. P. Gupta, Phys. Rev. B **23**, 6265 (1981).
[19] J. Jacobsen, L. P. Nielsen, F. Besenbacher, I. Stensgaard, E. Laegsgaard, T. Rasmussen, K. W. Jacobsen, and J. K. Norskov, Phys. Rev. Lett. **75**, 489 (1995).
[20] I. Meunier, G. Tréglia, J.-M. Gay, B. Aufray, and B. Legrand, Phys. Rev. B **59**, 10 910 (1999).
[21] G. Tréglia, B. Legrand, J. Eugéne, B. Aufray, and F. Cabané, Phys. Rev. B **44**, 5842 (1991).
[22] A. Barbier, Ph.D. thesis, Strasbourg, 1993.
[23] F. R. Nabarro, *Theory of Crystal Dislocations* (Oxford University Press, New York, 1967).
[24] J. E. Prieto, Ch. Rath, S. Muller, R. Miranda, and K. Heinz, Surf. Sci. **401**, 248 (1998).